



IV International Seminar on ORC Power Systems, ORC2017  
13-15 September 2017, Milano, Italy

## Radial Expander Design for an Engine Organic Rankine Cycle Waste Heat Recovery System

Fuhaid Alshammari, A.Karvountzis-Kontakiotis, A.Pesiridis\*, Timothy Minton

*Brunel University London, Department of Mechanical, Aerospace & Civil Engineering, Centre of Advanced Powertrain and Fuels (CAPF), Uxbridge UB8 3PH.*

---

### Abstract

It is commonly accepted that waste heat recovery technologies are significant contenders in future powertrain thermal management to further minimize fuel consumption and CO<sub>2</sub> emissions. Organic Rankine Cycle (ORC) systems are currently regarded as amongst the most potent candidates in recovering engine exhaust energy and converting it to electrical power. Crucial areas for the maximization of the efficiency of the ORC system are the appropriate selection of working fluid and the optimization of the expander design. In this study, a novel design methodology of a radial turbine expander for a heavy duty engine ORC waste heat recovery system is presented. The preliminary design of the radial turbine expander includes the development and utilization of an in-house 0/1D code that can be coupled with various organic fluids properties for the calculation of the basic expander geometry. The initial mean-line model for a 200kW-class Diesel engine application investigated produced a solution for a 20kW turbine with 73% isentropic efficiency. The preliminarily optimized expander geometry was used as an input in a detailed CFD code to further optimize rotor geometry. The rotor geometric optimization showed that by increasing exit tip radius by 10% and adopting a 54° back-swept blade design, the maximum isentropic efficiency achieved can exceed 83%.

© 2017 The Authors. Published by Elsevier Ltd.

Peer-review under responsibility of the scientific committee of the IV International Seminar on ORC Power Systems.

*Keywords:* Organic Rankine Cycle; Waste Heat Recovery; radial inflow expander; organic fluids; heavy duty diesel engine

---

### 1. Introduction

Demand for upscaling conventional powertrain hybridization has increased in recent years in order to meet with the stricter emission standards. The pressure to reduce CO<sub>2</sub> emissions results in demand for increased powertrain

\* Corresponding author. Tel.: +44(0)1895267901.

*E-mail address:* [apostolos.pesiridis@brunel.ac.uk](mailto:apostolos.pesiridis@brunel.ac.uk)

efficiency in diesel applications by adopting waste heat recovery technologies in future hybrid architectures, as more than half of the fuel energy in internal combustion engines is transformed to wasted heat [1].

Organic Rankine Cycle (ORC) systems are one of the most promising technologies which can be implemented to recover the wasted heat in low to medium heat sources due to their simplicity, technological maturity and reliability [2][3]. ORCs systems are Rankine cycle-based systems that use an organic working fluid instead of steam. Organic fluids present lower boiling points than steam which make them more suitable for low grade waste heat recovery systems. However, ORCs have usually low thermal efficiency levels due to the low working temperatures of the organic fluids. Some of the most promising outcomes to be expected from this technology include the results of Wang and Zhang [4] showing that the thermal efficiency of a six-cylinder diesel engine equipped with an ORC waste heat recovery system can be increased by 13.7% combined with a reduction in bsfc by 15.9%. The analysis of Vaja and Gambarotta [5] demonstrated that a 12% increase in the overall efficiency can be achieved with respect to the engine with no bottoming ORC.

To avoid further reductions in efficiency levels, it is essential to select and design the appropriate expansion machine. The expander is the most important component in the ORC power plant as it is responsible for power conversion [6]. Compared to positive displacement expanders, turboexpanders offer advantages such as compact structure, light weight and high efficiency [7]. Moreover, lubrication is not required when using turbo-machines which result in a cheaper and less complex design [8]. According to the open literature, radial inflow turbines showed better performance at low to medium heat grade sources compared to axial ones. Such turbines are capable of large enthalpy drops within a single stage while axial turbines require more stages. They are also more robust under increased blade loading, less sensitive to blade profile inaccuracies and easier to manufacture [9]. In addition to the expander, the properties of the working fluid have significant effects on the aerodynamic design of the expander [10] and the cycle thermal efficiency of the cycle.

In this study, the design methodology of a radial turbine expander for a heavy duty diesel engine exhaust waste heat recovery ORC system is presented. The preliminary design of the radial turbine expander includes the development and utilization of an in-house mean-line model that can be coupled with various organic fluids properties. The thermodynamic conditions of the ORC design point such as fluid temperature, pressure, mass flow rate and the desired expansion ratio are used in the mean-line model to calculate the basic expander geometry of the rotor, nozzles and volute. The mean-line model is used to optimize the expander geometry by maximizing the total-to-static isentropic efficiency, which is selected as the objective function. The target solution for this particular application is a 20kW turbine operating at a pressure ratio of 13 which is arrived at based on the required for maximization of the total-to-static efficiency. This target is achieved after the preliminary optimized expander geometry is used as an input in a detailed CFD code to further optimize the rotor geometry. CFD was utilized both to optimize the exit tip radius and to investigate the adoption of a 50° back-swept blade design.

#### Nomenclature

BK	Blockage factor	SST	Shear Stress Transport	Subscripts:
bsfc	brake specific fuel consumption	s	Entropy (KJ/Kg.K), vane spacing (m)	1-5 Stations across the turbine, Fig 1
C	Velocity (m/s)	T	Temperature	a axial
D	Diameter	U	Tip speed (m/s)	act actual
$f_t$	Friction factor	W	Relative velocity (m/s)	c curvature
h	Enthalpy (KJ/Kg)	Zr	number of rotor blades	hyd hydraulic
i	Incidence angle (degrees)	Zs	number of stator vanes	is isentropic
K	Discharge coefficient	Greek:		m meridional
L	length (m)	$\beta$	Relative blade angle	opt optimum
$\dot{m}$	Mass flow rate (kg/s)	$\eta$	Efficiency	r radial
M	Mach number (-)	$\rho$	Density (kg/m <sup>3</sup> )	
ORC	Organic Rankine Cycle	$\phi$	Flow coefficient (-)	
P	Pressure (KPa)	$\Psi$	Loading coefficient (-)	
r	Radius (m)	$\omega$	Rotational speed (rad/s)	

## 2. Modeling of Radial Inflow Turbine

The design process is initiated through the application of a mean-line code developed specifically for this purpose. This model is capable to provide a complete preliminary design of a turbine volute, stator and rotor. In order to start the mean-line methodology, the thermodynamic operating conditions at the volute inlet are specified from the initial engine and ORC system thermodynamic analysis as presented in Table 2.

### 2.1 General Stage Modeling

The full turbine stage and T-S diagram are shown in Fig. 1. Since the stagnation temperature and pressure are inputs to the mean-line model, the thermodynamic properties ( $\rho_{o1}, h_{o1}, s_{o1}$ ) are calculated from REFPROP [11]. The isentropic enthalpy  $h_{5s}$  is calculated from total inlet entropy and static, isentropic exit pressure ( $s_{o1}$  and  $P_{5s}$ ), assuming  $s_{5s} = s_{o1}$  and  $P_5 = P_{5s}$ , where  $P_5$  is determined from the user defined pressure ratio. The isentropic and actual enthalpy drops, and turbine power output can be obtained using the following equations:

$$\Delta h_{is} = h_{o1} - h_{5s} \quad (1)$$

$$\Delta h_{act} = \eta_{ts} \Delta h_{is} \quad (2)$$

$$W_{out} = \dot{m} \Delta h_{act} \quad (3)$$

$$W_{out} = U_4 C_{\theta 4} - U_5 C_{\theta 5} \quad (4)$$

### 2.2 Rotor Modeling

Rotor is the most significant component in the turbine stage since the work transfer occurs in this region. The design of the rotor is performed following a procedure based on Moustapha et al. [12]. The rotor is modeled based on two non-dimensional parameters, the loading coefficient  $\Psi$  and flow coefficient  $\phi$ , which are described in equations (5) and (6) respectively.

$$\Psi = \frac{\Delta h_{act}}{U_4^2} \quad (5)$$

$$\phi = \frac{C_{m5}}{U_4} \quad (6)$$

The loading coefficient  $\Psi$  and flow coefficient  $\phi$  are optimized using the optimization algorithm and the user defined constraints. Then, the rotational speed  $U_4$  and the meridional velocity  $C_{m5}$  at the rotor outlet can be calculated and the velocity triangles at the rotor leading edge can be defined (Fig. 1).

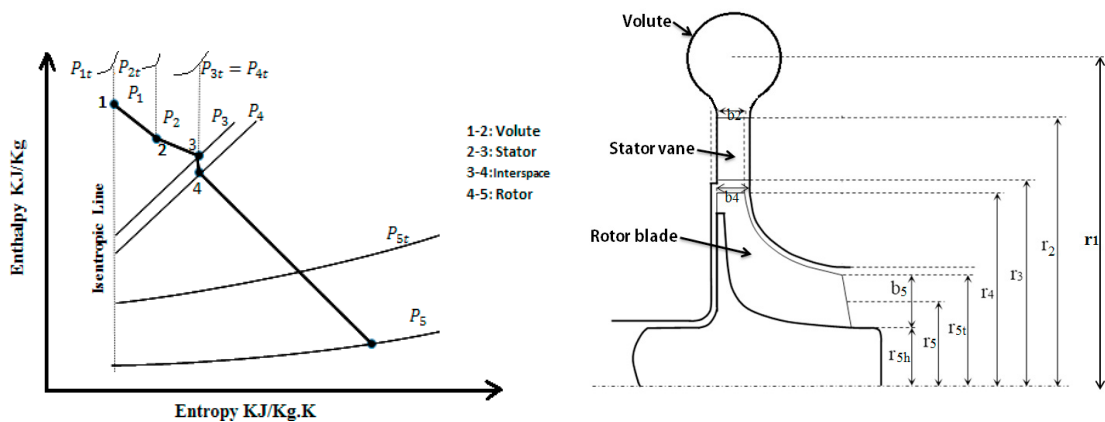


Fig. 1. (left) T-s diagram of the full stage; (right) geometric parameters of turbine stage

Equation (4) shows that the maximum turbine power output is achieved when the tangential velocity at the rotor exit ( $C_{\theta 5}$ ) is minimized. In many of the conventional methodologies, this value is considered as zero. However, in real applications, the swirl at the turbine outlet is not avoidable due to the complex secondary flow in this region. In the current work, the tangential velocity at the rotor exit  $C_{\theta 5}$  was obtained by combining the Euler

turbomachinery equation (4) with the definition of the total-to-static efficiency equation (7) as presented in equation (8). The velocity triangle at the rotor exit can be calculated using appropriate trigonometry.

$$\eta_{ts} = \frac{h_{01} - h_{05}}{h_{01} - h_{5s}} \quad (7)$$

$$C_{\theta 5} = \frac{U_4 C_{\theta 4} - (h_{01} - h_{05})}{U_5} \quad (8)$$

### 2.3 Stator and Volute Modeling

The main function of the nozzle vanes is to provide the appropriate flow guidance, flow acceleration and to remove any circumferential non-uniformity. The stator element is modeled on a procedure based on Aungier [13]. The design procedure of the nozzle vanes are performed iteratively and a blade thickness distribution on a parabolic-arc camber-line is imposed.

Volute modeling includes the calculation of the primary volute passage area and its mean radius by using the mass conservation and the angular momentum equations.

### 2.4 Loss Modeling

The loss model in this study is expressed in terms of enthalpy drop and explained below for each of the loss components of the turbine. A first assumption of the total-to-static efficiency is required in order to proceed with the preliminary design of the turbine stage. Then, the new value of the efficiency is calculated after considering turbine losses (equations 9 – 12). The losses model is presented in detail in [12] including their sources.

- Incidence loss

$$\Delta h_{incidence} = \frac{1}{2} [W_4 \sin(\beta_4 - \beta_{4,opt})]^2 \quad (9)$$

- Passage Loss

$$\Delta h_{passage} = \frac{1}{2} \left( 2f_t \frac{L_{hyd}}{D_{hyd}} \bar{W}^2 + \frac{r_4 C_4^2}{r_c Z_r} \right) \quad (10)$$

- Tip Clearance Loss

$$\Delta h_{tip} = \frac{U_4^3 Z_r}{8\pi} (K_a \varepsilon_a C_a + K_r \varepsilon_r C_r + K_{a,r} \sqrt{(\varepsilon_a \varepsilon_r C_a C_r)}) \quad (11)$$

- Exit Energy Loss

$$\Delta h_{exit} = \frac{1}{2} C_5^2 \quad (12)$$

The mean-line model provides a solution for isentropic efficiency and power output of the expander through an iterative procedure. An isentropic efficiency is assumed and based on this the calculations of the rotor, stator volute and losses are performed, which result to a new isentropic efficiency. The final solution is reached when the initially assumed efficiency converged with the final solved isentropic efficiency.

The mean-line model then proceeded to maximize the objective function, which in this study is the isentropic efficiency. This objective function is further constrained by user defined constraints such as radius ratio  $\frac{r_2}{r_3}$ , absolute flow angle at rotor inlet  $\alpha_4$  and blade height  $b_4$ . As a result, the optimization module returns the optimum expander geometry for a given design point.

## 3. Results and Discussion

### 3.1 Powertrain System

The heavy duty diesel engine used in this study is a 7.25l Yuchai engine. Table 1 provides the basic engine specification and operating characteristics. The detailed characteristics of the powertrain system, the selection of the proper working fluid and the modeling of the ORC system are explained in the previous work of the authors [14]–

[18]. This study is mainly focused on the design of the radial inflow expander, when the ORC system operates under design conditions. Other works such as the performance of the proposed ORC system under off-design conditions and the experimental validation of this system are under development by the authors.

Table 1: Engine specification and main operating characteristics

Displaced Volume	7255cc
Stroke	132 mm
Bore	108 mm
Compression Ratio	17.5:1
Number of cylinders	6
Number of valves	4
Maximum torque	1100Nm @ 1400-1600rpm
Maximum power	206kW @ 2300rpm
Optimum bsfc	$\leq 205\text{g/kWh}$

### 3.2 Preliminary Expander Design

The model presented in section 2 is coupled with the MATLAB optimization toolbox to define the optimum expander characteristics using as an objective function the total-to-static isentropic efficiency. The main geometrical and performance parameters of the full turbine stage are shown in Table 2 and the schematic diagram of the full stage is shown in Fig. 1.

Table 2: Basic geometric and performance parameters of the turbine stage (Baseline)

Input conditions		Rotor		Stator		Volute		Performance	
T1	471.5 (K)	r4 (m)	0.034	r2 (m)	0.0445	r1 (m)	0.051	Power (kW)	18
P1	1690 kPa	b4 (m)	0.0034	b2 (m)	0.0034			$\eta_{t-s}$ (%)	72.5
PR	13	r5t (m)	0.02	r3 (m)	0.035			$\phi$	0.98
m	0.923 (kg/s)	r5h (m)	0.008	b3 (m)	0.0034			$\Psi$	0.24
		b5 (m)	0.015	Zs (-)	17			Zr	15
		$\beta_{4,blade}$ (deg)	0	$\alpha_3$ (deg)	79			Zs	17
		$\alpha_4$ (deg)	77	M3	1.6			Rotational speed (rpm)	40,000
		$\beta_4$ (deg)	33	P3 (kPa)	432.21				
		P4 (kPa)	378						
		Mrel,5	0.72						

One of the main aims of this study is to increase the efficiency of the turbine by optimizing the variable inlet conditions. One of the variables that showed a substantial effect on turbine performance is the rotor exit tip radius  $r_{5,tip}$ . In order to study the effect of this parameter, it is set as an input parameter in the turbine model. However, its value is constrained by equation (13), as presented in Aungier [13].

$$r_{5,tip} \leq 0.78 r_4 \quad (13)$$

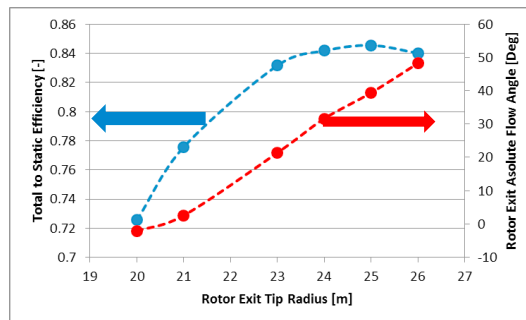


Fig. 2: Influence of Exit Tip Radius on Turbine performance and Exit angle

The influence of  $r_{5,tip}$  is shown in Fig. 2. It is illustrated that turbine efficiency increases substantially as  $r_{5,tip}$  increases. The total-to-static efficiency increases by 16% as the exit tip radius  $r_{5,tip}$  is increased by 25% compared

to the baseline turbine. As  $r_{5,tip}$  increases, the tip clearance loss, mainly the radial tip clearance, decreases and therefore higher turbine performance is achieved. Moreover, the tangential component of the velocity  $C_{\theta 5}$  decreases with increasing exit tip radius which results in higher specific work according to the Euler equation. However, it is worth noting that increasing the exit tip radius  $r_{5,tip}$  will result in higher absolute flow angles at the rotor trailing edge. This, in turn, will result in a flow deviation at the rotor trailing edge.

Another important design parameter is the inlet blade angle  $\beta_{blade}$ . Since the operating temperature of the model is less than 200° C, it is possible to adopt a non-zero blade angle  $\beta_{blade}$  at the rotor inlet without considering the bending stresses as in conventional turbines. Fig. 3a presents a schematic comparison of radial and non-radial blades. Increasing the inlet blade angle results in a higher tangential velocity which, based on the Euler equation (equation 4), results in higher specific work. Hence, higher efficiency can be achieved as shown in Fig. 3b, where isentropic efficiency is increased by approximately 1.5% by changing the conventional blade (0° blade angle) to 54°. However, increasing the blade angle to higher values (> 54°) will result in excessive blade curvature and hence higher secondary losses. Therefore, the efficiency deteriorates with any further increase in the blade angles as can be seen in Fig. 3b.

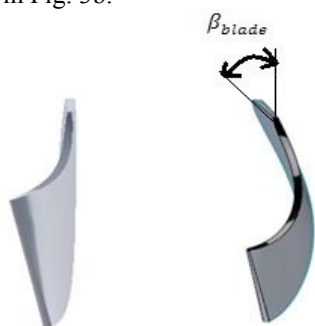


Fig. 3a: (left) radial blade (right) non-radial blade

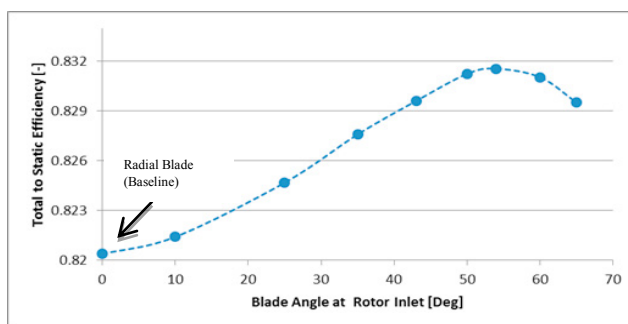


Fig. 3b: (left) Effect of inlet blade angle on turbine performance

The effects of the two parameters  $\beta_{blade}$  and  $r_{5,tip}$  on the baseline design are shown in Fig. 4a. The total-to-static efficiency increases from 73 to 82% by increasing the exit tip radius by 9.5%. The performance is further improved by adopting a 54° back-swept blade angle whereby the efficiency reaches 83.5%. The power output also increased correspondingly from 18 kW to 20kW. The final turbine stage is given at Fig. 4b.

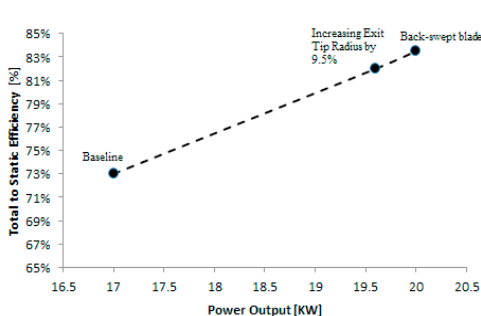


Fig. 4a: Efficiency Improvement of the radial turbine

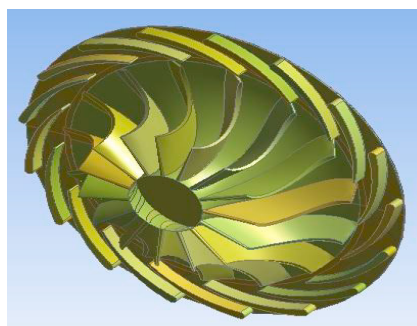


Fig. 4b: Turbine stage after improvement

### 3.3 Detailed Expander Design

The purpose of the computational fluid dynamic (CFD) investigation is to confirm that the predicted rotor aerodynamics are sound and that no major flow loss mechanisms exist, necessitating further action. The 3D parts are generated using Ansys BladeGen tool. After building the geometries of the stator vanes and rotor blades, the final CAD is exported into Ansys Turbogrid to generate hexahedral meshes of sufficient quality while preserving the underlying geometry. The meshed parts (Fig. 5) are then exported into ANSYS CFX-Pre to set the boundary conditions and the physical properties of the organic fluid. Table 3 below presents the meshing properties and boundary conditions used in the simulation study. As pitch ratio between the rotor and stator is close to 1, a single

stator vane and single rotor blade passage are considered in the simulation and a periodic symmetry is set. A steady state simulation is carried out with SST as the turbulence model and mixing plane (stage) is assumed at the interface between the stator outlet and the rotor inlet.

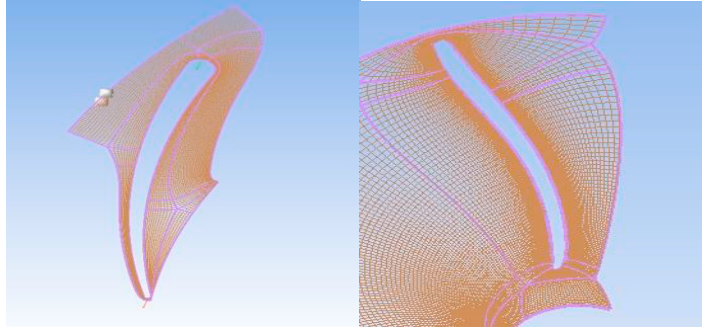


Fig. 5: (left) Meshed stator vane and rotor blade (right) using ANSYS TurboGrid

Table 3: Mesh properties and boundary conditions in the CFD analysis

	Number of nodes	Number of elements
<b>Stator</b>	671520	620685
<b>Rotor</b>	300000	270290
Boundary Conditions		
T01(K)	P01(KPa)	P5 (KPa)
471.5	1690	130

Fig. 6 presents the pressure, velocity and Mach number contours along the turbine stage. As shown, the distribution of pressure is uniform and exhibits good flow features. Moreover, it can be seen from pressure contours that the working fluid generally follows the radial circumferential plane. However, there is a high pressure area at the rotor inlet resulting in a higher blade loading in this region which however is not substantial enough to necessitate further change in local blade curvature for the reasons outlined earlier in the discussion on results at Fig.3. Fig. 6 also presents the velocity streamlines across the turbine stage. The streamlines orientation seems to confirm a smooth passage transition through stator vane and rotor blade with no discernible secondary flow build-up occurring in the blade passages. However, Mach number at stator exit is quite high, which confirms the 1D results in Table 2. That is normal in ORC turbines due to the low values of speed of sound and the extremely high pressure ratio. The maximum total to static efficiency reached in CFD simulation is 81.3%. This calculated value is 2.2% lower compared to the preliminary design value. The result can be explained from the fluid equation of state (EOS) integrated in ANSYS. According to White, there is a discrepancy up to 4% in the enthalpy drop when applying the ANSYS equation of state compared to REFPROP [19].

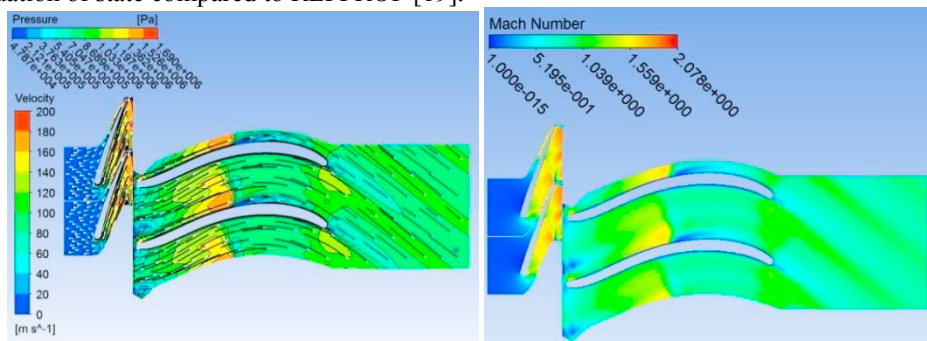


Fig. 6: (left) Pressure and velocity distribution (right) Mach number distribution through the stage.

## 4 Conclusions

This study presents a novel, hybrid design methodology of a radial turbine expander that is employed in an engine exhaust waste heat recovery ORC system. The preliminary design of the radial turbine expander was enabled through the development and utilization of an in-house mean-line model. In addition, a detailed CFD analysis was performed to validate the mean-line modeling results.

The presented mean-line modeling of the radial expander focused on two main design parameters, namely, the rotor inlet blade angle  $\beta_{blade}$  and rotor exit tip radius  $r_{5,tip}$ . It was found that by increasing  $r_{5,tip}$  by 9.5% compared to the baseline, the isentropic efficiency ( $\eta_{ts}$ ) increases from 73% to 82%. Furthermore, increasing  $\beta_{blade}$  from 0° to 54°, a further improvement of 1.5% could be obtained on the total-to-static efficiency. The eventual 83.5% isentropic efficiency achieved indicates that this radial expander is approaching its limiting performance for this size class of radial expander.

Preliminary CFD simulations were performed to investigate the flow field within the turbine stage. The results showed that the generally smooth flow transitions occur from the inlet of the stator vane to the outlet of the rotor blade. The predicted total-to-static efficiency of the turbine using CFD was found 2.2% lower than the 1D modeling. A more detailed and extensive CFD study will be conducted in the future in order to capture any secondary flows in critical stations such as the interspace between the stator and rotor, which will be then used to attempt to obtain further efficiency gains from the design.

### Acknowledgements

The authors would like to acknowledge the financial support of Innovate UK to this project (ref. TS/M012220/1).

### References

- [1] X. X. Zhang, K. Zeng, and M. G. He, "New Technology of Thermodynamic Cycle for Waste Heat Recovery of Vehicle Gasoline Engine," *2009 Asia-Pacific Power and Energy Engineering Conference*, pp. 1–6, 2009.
- [2] Y.-R. Lee, C.-R. Kuo, and C.-C. Wang, "Transient response of a 50 kW organic Rankine cycle system," *Energy*, vol. 48, no. 1, pp. 532–538, Dec. 2012.
- [3] D. Fiaschi, G. Manfrida, and F. Maraschiello, "Thermo-fluid dynamics preliminary design of turbo-expanders for ORC cycles," *Appl. Energy*, vol. 97, pp. 601–608, 2012.
- [4] H. Z. Hongjin Wang, "Performance Analysis of Waste Heat Recovery with a Dual Loop Organic Rankine Cycle System for Diesel Engine," in *3rd International Seminar on ORC Power Systems, October 12-14, 2015, Brussels, Belgium*.
- [5] I. Vaja and A. Gambarotta, "Internal Combustion Engine (ICE) bottoming with Organic Rankine Cycles (ORCs)," *Energy*, vol. 35, no. 2, pp. 1084–1093, Feb. 2010.
- [6] Y. M. Yang, S. P. Byung, S. W. Lee, and D. H. Lee, "Development of a Turbo-generator for ORC System with Twin Radial Turbine and Gas Foil Bearing," in *3rd International Seminar on ORC Power Systems, October 12-14, 2015, Brussels, Belgium*.
- [7] K. Rahbar, S. Mahmoud, R. K. Al-Dadah, and N. Moazami, "Modelling and optimization of organic Rankine cycle based on a small-scale radial inflow turbine," *Energy Convers. Manag.*, vol. 91, pp. 186–198, 2015.
- [8] Andreas P. Weiß, "VOLUMETRIC EXPANDER VERSUS TURBINE – WHICH IS THE BETTER CHOICE FOR SMALL ORC PLANTS," in *3rd International Seminar on ORC Power Systems, October 12-14, 2015, Brussels, Belgium*, 2015, pp. 1–10.
- [9] E. Sauret and A. S. Rowlands, "Candidate radial-inflow turbines and high-density working fluids for geothermal power systems," *Energy*, vol. 36, no. 7, pp. 4460–4467, 2011.
- [10] Y. Li and X. Ren, "Investigation of the organic Rankine cycle (ORC) system and the radial-inflow turbine design," *Appl. Therm. Eng.*, vol. 96, pp. 547–554, Mar. 2016.
- [11] E. Lemmon, M. Huber, and M. McLinden, "NIST Standard Reference Database 23: Reference Fluid Thermodynamic and Transport Properties-REFPROP, Version 9.0, National Institute of Standards and Technology, Standard Reference Data Program, Gaithersburg, Maryland, USA." 2010.
- [12] H. Moustapha, M. F. Zelesky, N. C. Baines, and D. Japikse, *Axial and Radial Turbines*, 1st ed. White River Junction: Concepts NREC, 2003.
- [13] R. H. Aungier, *Turbine aerodynamics: Axial-flow and radial-inflow turbine design and analysis*, 1st ed. New York, 2006.
- [14] A. Karvountzis-Kontakiotis, A. Pesiridis, F. Alshammari, et al., "Effect of an ORC Waste Heat Recovery System on Diesel Engine Fuel Economy for Off-Highway Vehicles." SAE International, 2017.
- [15] A. Karvountzis-Kontakiotis, F. Alshammari, and A. Pesiridis, "Design of Radial Turbine Expanders for Organic Rankine Cycle, Waste Heat Recovery in High Efficiency, Off-Highway Vehicles," in *3rd Annual Engine ORC Consortium Workshop, Queens University Belfast, UK, 14-16 September 2016*.
- [16] A. Karvountzis-Kontakiotis, F. Alshammari, A. Pesiridis, B. Franchetti, I. Pasmazoglou, and L. Tocci, "Variable Geometry Turbine Design for Off-Highway Vehicle Organic Rankine Cycle Waste Heat Recovery," in *THIESEL 2016 Conference on Thermo-and Fluid Dynamic Processes in Direct Injection Engines, Valencia, Spain (2016)*.
- [17] F. Alshammari, A. Karvountzis-Kontakiotis, and A. Pesiridis, "Radial turbine expander design for organic rankine cycle, waste heat recovery in high efficiency, off-highway vehicles," in *3rd Biennial International Conference on Powertrain Modelling and Control (PMC 2016), 7-9 September 2016, Loughborough, UK, (2016)*.
- [18] B. Franchetti, A. Pesiridis, I. Pasmazoglou, E. Sciubba, and L. Tocci, "Thermodynamic and technical criteria for the optimal selection of the working fluid in a mini-ORC," in *ECOS 2016 - the 29th International Conference on Efficiency, Cost, Optimization, Simulation and Environmental Impact of Energy Systems June 19-23, 2016, Portorož, Slovenia, (2016)*.
- [19] M. White, "The design and analysis of radial inflow turbines implemented within low temperature organic Rankine cycles," PhD thesis. City University London, 2015.